Reprinted from

JOURNAL OF THE PHYSICAL SOCIETY OF JAPAN

JOURNAL OF THE PHYSICAL SOCIETY OF JAPAN

http://jpsj.jpap.jp/

FULL PAPER

Theoretical Study of Discharge in a Nonlinear Medium

Shogo Matsumoto and Takashi Odagaki

J. Phys. Soc. Jpn. **88**, 034704 (2019)

Journal of the Physical Society of Japan **88**, 034704 (2019)
https://doi.org/10.7566/JPSJ.88.034704

Theoretical Study of Discharge in a Nonlinear Medium

Shogo Matsumoto[1] and Takashi Odagaki[2*]

[1]*Tokyo Denki University, Hatoyama, Saitama 350-0394, Japan*
[2]*RISE Inc., Kyoto 603-8346, Japan*

(Received November 7, 2018; accepted January 15, 2019; published online February 8, 2019)

Exploiting a nonlinear resistor network on a square lattice in two dimensions, we investigate discharge when two opposite sides of the lattice are subjected to a fixed voltage difference. We assume that each site can take one of three states; freshly-ionized (F-site), aged-ionized (A-site), and neutral (N-site) states. An F-site is rejuvenated with some probability, and when it is not rejuvenated, it becomes an A-site. An A-site can be rejuvenated back to an F-site or it can be neutralized. Otherwise, it stays as an A-site with older age. An N-site can be ionized with some probability to become an F-site. Each site is ionized with a probability which is an increasing function of the strength of the electric field. The resistivity between two ionized sites is assumed to be 10^{-6} times smaller than the original resistivity. We obtain the current between two electrodes at the opposite edges of the lattice and the fraction of ionized sites as functions of the potential difference by a Monte Carlo simulation. We find that as the potential difference is increased, the system changes its state discontinuously from the non-conductive to the conductive state, similar to the first-order phase transition. We show that non-conductive and conductive states can coexist at a given applied potential difference. We analyze the transition on the basis of a mean field approach and find that the local effect of a cluster structure of ionized sites on ionization and rejuvenation is important for the transition and that the discontinuous transition is induced by rejuvenation of ionized sites.

1. Introduction

In an inhomogeneous electric field such as the field produced by an applied field between a needle and a planar electrode, dielectric breakdown occurs locally which is called a corona discharge. The structure of the discharge is called a streamer since it expands like fibrous roots. Streamer discharges have the structure with detouring and bifurcation like the lightning. It has been argued that streamer discharges are caused by the so-called α-process which is a simple ionization of gas molecules by accelerated electrons. However, it is not known why discharges caused by the α-mechanism produces the complex structure.

Gas discharge between electrodes occurs when the applied voltage is increased above a critical value. It has been observed in an accelerator that the probability of breakdown when pulsed voltages are applied depends on the external field and the breakdown probability is not a step function of the voltage.[1)] The voltage dependence of breakdown probability has also been observed in SF_6 under an applied AC voltage.[2)] Although breakdown occurs when the applied voltage is larger than the withstand voltage, the breakdown probability depends on applied electric field and therefore breakdown does not always occur at the same condition.

Since a laser pulse can propagate over a long distance and produces a plasma channel, triggering and guiding of discharge by an ultra-short pulse laser have attracted attention.[3)] Inducing discharge by the laser is important for applications such as the lightning control and protection.

A long gap discharge induced by laser plasma channels has been observed.[4)] This indicates that discharge might be considered as a percolation process of plasma region which has high electrical conductivity.

Discharges have been investigated as a fractal because of the structure with self-similarity.[5,6)] In addition, Kishimoto et al. reproduced the structure of discharge by a kinetic simulation including atomic and relaxation processes for a lightning process with the particle-in-cell (PIC) method which has been widely used in simulating plasma dynamics.[7)] In the PIC simulation, many tiny ionization spots appear in the entire system before an avalanche-like propagation of the spots occurs. Since micro-scale discharges are triggered between neighboring spots when the packing fraction of the spots exceeds a certain value, the process looks similar to that of percolation process.

Sasaki et al. exploited a resistor network and the percolation theory[8)] to understand the discharge. In their approach, the space between planar electrodes is divided into coarse-grained cells which take one of two states, either ionized or neutral, and nearest neighbor cells are connected by a resistor which can be conductive or non-conductive depending on the states of the cells. Namely a resistor becomes conductive when and only when two cells connected by the resistor are ionized. A neutral cell is ionized by a probability $p_{\rm ion}$ given by

$$p_{\rm ion} \propto |\boldsymbol{E}_i|^{\alpha}, \tag{1}$$

where $\boldsymbol{E}_i$ is a local electric field, and α is a parameter. Sasaki et al. have investigated success rate of laser guiding of the discharge which depends on laser patterns and ionization parameter α. They found a transition similar to the percolation, which is a continuous transition, when the fraction of ionized cells is increased. However, the discharge has not been investigated as a transition phenomenon.[9)]

In a previous paper,[10)] we introduced a nonlinear resistor network model and reported that the nonlinear model shows a mixed behavior of ordinary and directional percolation processes, and the scaling relations are satisfied by exponents obtained from the cluster distribution. Namely, the growth of clusters in the model is the same as that in the ordinary percolation process. However, the critical behavior of the current percolation is different from that of the cluster distribution. This indicates that discharge occurs before the ionized regions expand sufficiently large in the system owing to the nonlinearity of ionization and the local growth of ionized regions.

From the observations of discharges described above, we can summarize the characteristics of the discharge as follows:

(1) The scale universality for structure formation
Although streamer discharges differ from the lightning in the scale, the structures are similar to one another and they are formed mainly by the α-mechanism.

(2) Discontinuous transition from non-conductive to conductive state when the voltage is increased
Since the breakdown does not always occur at the same condition, there are two states, one is non-conductive and the other is conductive at the same condition. Therefore, it is expected that the state changes discontinuously by the discharge when the voltage between electrodes is increased.

In previous researches, the discontinuous nature of discharge has not been paid much attention.

In this paper, we investigate the discharge as a transition phenomenon using coarse-grained models in consideration of the universality of structure formation. In Sect. 2, we explain the resistor-network model in which each site can take three different states, where ionized region can be neutralized and rejuvenated. In Sect. 3, we present the results of Monte Carlo simulation and show that the discharge accompanies a discontinuous transition. We discuss the details of the discontinuous transition in Sect. 4 and the origin of the transition in Sect. 5. In order to strengthen our argument, we show in Sect. 6 the theoretical analysis of the transition on the basis of the mean field approach. Conclusion is given in Sect. 7.

2. Nonlinear Resistor Network Model with Three States

We employ the coarse-grained model [Fig. 1(a)],[8,10] and modify it so that we can discuss the dependence of discharge on the potential difference between two electrodes. In the coarse-grained model employed in previous works,[8,10] it was assumed that each site can take one of two states; neutral and ionized. However, when the energy of an ionized site is sufficiently high, it takes some time before it is neutralized by recombination since it must lose its energy for recombination. Therefore, during this process, an ionized site can be excited again to a higher energy state. It is, thus, natural to assume that a site can take one of three states; freshly-ionized (F-site), aged-ionized (A-site), and neutral (N-site) states. We note that the difference between freshly-ionized and aged-ionized states is in the energy of the site. In high energy media (for example their temperature is high because of Joule heat caused by the local high-current), recombination of ionized states is inhibited. We assume that an F-site is rejuvenated with probability a and when it is not rejuvenated with probability $1-a$, it becomes an A-site. An A-site can be rejuvenated back to an F-site with probability b or it can be neutralized with probability $(1-b)g$. Otherwise it will stay as an A-site with older age with probability $(1-b)(1-g)$. An N-site can be ionized with probability f. Figure 1(b) shows schematically the elementary processes and the branching ratios.

The detail of resistor network is the same as Sasaki's model.[8] The adjacent sites are connected by a resistor which is conductive when sites at both ends of the resistor are ionized (F-site or A-site) and non-conductive otherwise. The resistivity of non-conductive state is set to r_0 and that of conductive state is $10^{-6}r_0$. One set of edges is subjected to a potential difference V and the other set of edges satisfies a periodic boundary condition.

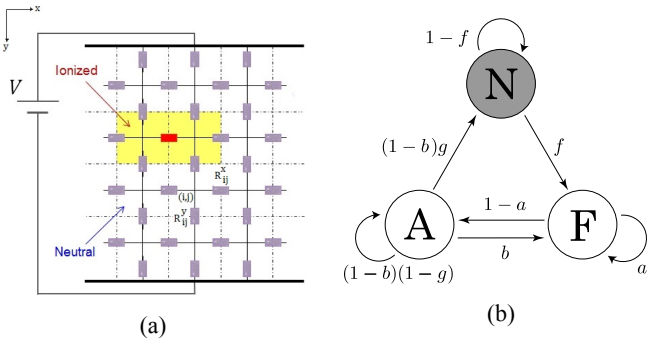

Fig. 1. (Color online) (a) A coarse-grained model and the corresponding resistor network in two dimensions.[8] (b) Transition routes and branching ratios among freshly-ionized (F), aged-ionized (A), and neutral (N) states.

3. Monte Carlo Simulation of the Coarse-grained Model

We exploit the Townsend form[11] as the normalized ionization probability f,

$$f(E_i) = \exp(-E_0/E_i), \tag{2}$$

where E_i is the electric field at site i, E_0 is an electric field characterizing the ionization of a medium. Here, $(V_0 \equiv E_0(N+1)\ell$ is the reference voltage when the mean electric field in the resistor network coincides with E_0, and ℓ is the lattice constant serving as the scale of the length. The normalized recombination probability g is assumed to be

$$g(\tau) = 1 - e^{-t_0/\tau}, \tag{3}$$

where t_0 is the time scale of one Monte Carlo step. Note that τ represents characteristics of the media, that is the recombination rate is small when τ is large. The probabilities, a and b, of rejuvenation of an F- and an A-site are assumed to be the same as f. Our Monte Carlo simulation proceeds as follows: At the beginning, all sites are set to be neutral and all resistors are assumed to be non-conductive. In order to obtain the potential at each site and the current flowing on each bond, we solve the following circuit equations:

$$I^x_{ij}R^x_{ij} = V(i,j) - V(i+1,j), \tag{4}$$

$$I^y_{ij}R^y_{ij} = V(i,j) - V(i,j-1) \tag{5}$$

and

$$I^x_{i-1j} + I^y_{ij-1} = I^x_{ij} + I^y_{ij}, \tag{6}$$

where each site is labelled by two indexes (i,j), the electric potential at (i,j) is written as $V(i,j)$, the resistors between the sites (i,j) and $(i+1,j)$ and between the sites (i,j) and $(i,j+1)$ are denoted by R^x_{ij} and R^y_{ij}, respectively, and the current between (i,j) and $(i+1,j)$ and between (i,j) and $(i,j+1)$ are denoted by I^x_{ij} and I^y_{ij}, respectively.

We also calculate the strength of the electric field at each site $E^2(i,j) = E^2_x(i,j) + E^2_y(i,j)$ from the difference of the potentials, where the electric fields $E_x(i,j)$ and $E_y(i,j)$ at (i,j) are obtained by

$$E_x(i,j) = \frac{V(i-1,j) - V(i+1,j)}{2\ell}, \tag{7}$$

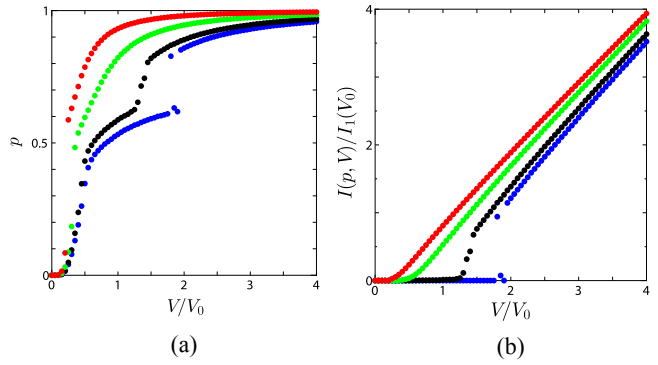

Fig. 2. (Color online) The fraction of ionized sites (a) and the current (b) as a function of applied potential difference for various relaxation times; the lowest series of dots (blue): $\tau/t_0 = 0.5$, the second lowest series of dots (black): $\tau/t_0 = 1.0$, the second series from the top (green): $\tau/t_0 = 3.0$, and the top series of dots (red): $\tau/t_0 = 10.0$.

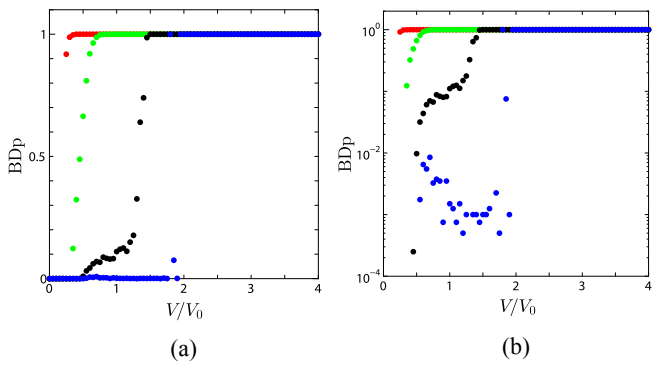

Fig. 3. (Color online) Breakdown probability in linear scale (a) and logarithmic scale (b) as a function of applied potential difference in various relaxation times; the lowest series of dots (blue): $\tau/t_0 = 0.5$, the second lowest series of dots (black): $\tau/t_0 = 1.0$, the second series from the top (green): $\tau/t_0 = 3.0$, and the top series of dots (red): $\tau/t_0 = 10.0$.

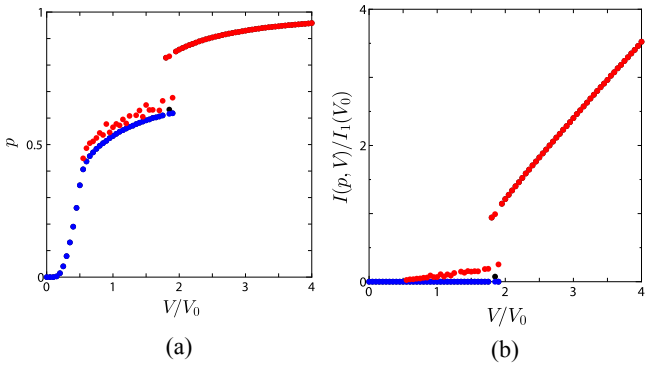

Fig. 4. (Color online) The fraction of ionized sites (a) and the current (b) as a function of applied potential difference for $\tau/t_0 = 0.5$ averaged among the same state individually; the lower series of dots (blue: only in $V/V_0 \leq 2$): non-conductive state, the upper series of dots (red): conductive state.

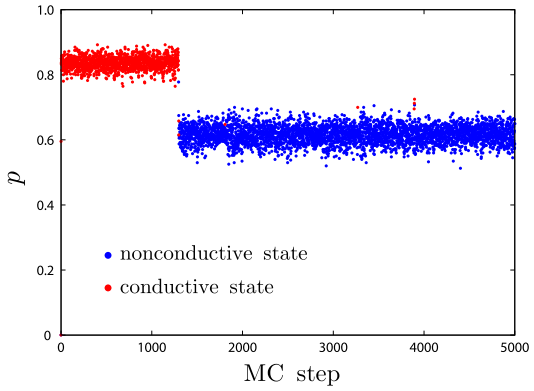

Fig. 5. (Color online) Time evolution of the fraction of ionized sites at $V/V_0 = 1.90$ for $\tau/t_0 = 0.5$. Most of the upper portion corresponds to the conductive states and most of the lower portion is the non-conductive state. In the conductive state, there is at least one cluster of ionized sites connecting both electrodes.

$$E_y(i,j) = \frac{V(i,j-1) - V(i,j+1)}{2\ell}. \tag{8}$$

After completing these calculations, we update the state of each site according to the branching ratios shown in Fig. 1(b).

This completes one Monte Carlo step. We repeated 5.0×10^3 steps of the elementary Monte Carlo process and obtained physical quantities from the time average, taking samples from the last 4.0×10^3 steps, for various potential differences.

4. Discontinuous Transition

4.1 Coexistence of conductive and non-conductive states

Figures 2 and 3 show the V dependence of the fraction of the ionized sites, the current flowing from the electrode, and the breakdown probability for $\tau/t_0 = 0.5$, 1.0, 3.0, and 10.0 in a 20×20 square lattice. We defined the breakdown probability as the frequency of a conductive state appearing during Monte Carlo steps. From the semi-logarithm plot of the breakdown probability [Fig. 3(b)], the breakdown probability can well be regarded to linearly increase with the voltage, which is the same behavior observed in experiments.

There is a discontinuous transition from non-conductive to conductive state when the potential difference is increased. Since the transition appears prominently in shorter relaxation time, we analyze the transition for $\tau/t_0 = 0.5$ in detail.

We averaged physical quantities among the same states which are shown in Fig. 4. From $V/V_0 = 0.5$ to 1.8, there are few conductive states which remain the state transiently so that the events have no appreciable effect on the average. Although the system is maintained in only conductive state at higher voltage difference, we found that the system is sustained either conductive or non-conductive state around $V/V_0 \simeq 2.0$.

Figure 5 shows the time evolution of the fraction of ionized sites at $V/V_0 = 1.90$. There are two stable states at the same voltage difference. Therefore, the discontinuous transition from non-conductive to conductive state is similar to a first-order phase transition because non-conductive and conductive states coexist at some applied potential difference.

4.2 Cluster structure and local electric fields

To clarify the property of conductive and non-conductive states, we investigated the cluster structure and the electric potential in each state at the voltage where the two states can be stable. Figure 6 shows the cluster structure and the electric

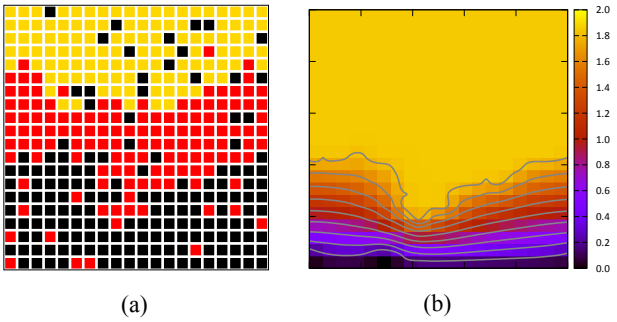

Fig. 6. (Color online) The cluster structure (a) and the electric potential (b) of a non-conductive state at $V/V_0 = 1.90$ for $\tau/t_0 = 0.5$. Black squares are neutral sites, dark grey (red in color) squares are aged-ionized sites, and light grey (yellow in color) squares are freshly-ionized sites, respectively. The potential is colored in ten scales by its height.

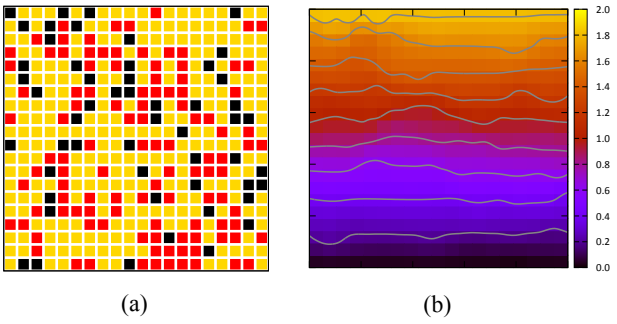

Fig. 7. (Color online) The cluster structure (a) and the electric potential (b) of a conductive state at $V/V_0 = 1.90$ for $\tau/t_0 = 0.5$. Black squares are neutral sites, dark grey (red in color) squares are aged-ionized sites, and light grey (yellow in color) squares are freshly-ionized sites, respectively. The potential is colored in ten scales by its height.

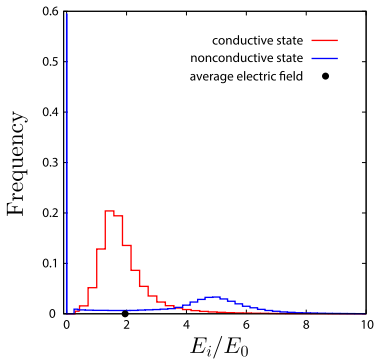

Fig. 8. (Color online) Histogram of local electric fields of a conductive state (the curve with a single-peak around $E_i/E_0 = 2$) and a non-conductive state (the curve with a small peak around $E_i/E_0 = 5$ and a δ-peak at $E_i/E_0 = 0$) at $V/V_0 = 1.90$ for $\tau/t_0 = 0.5$.

potential of a non-conductive state and Fig. 7 shows those of a conductive state. In the non-conductive state, the local electric field of ionized sites is weak and that of neutral sites is strong. On the other hand, local electric field of each site is comparable in the conductive state.

Figure 8 shows a histogram of local electric fields in the coexisting states at $V/V_0 = 1.90$. As can be seen in Fig. 8, local electric fields in the conductive state distribute around the strength of the external electric field. In the non-conductive state, local electric fields are distributed around

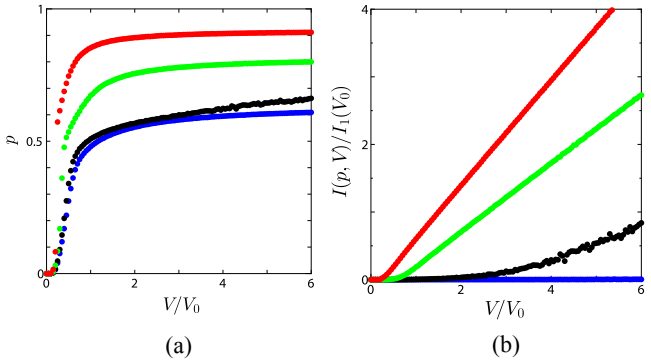

Fig. 9. (Color online) The fraction of ionized sites (a) and the current (b) as a function of applied potential difference for various relaxation times where ionized sites cannot be rejuvenated; The lowest series of dots (blue): $\tau/t_0 = 0.5$, the second lowest series of dots (black): $\tau/t_0 = 1.0$, the second series from the top (green): $\tau/t_0 = 3.0$, and the top series of dots (red): $\tau/t_0 = 10.0$.

two values: One is zero and the other is twice as high as the applied electric field. Therefore, we found that the distribution of local electric fields is different between the conductive and non-conductive states.

5. Mechanism for Coexistence of Conductive and Non-conductive States

We can understand why the conductive and non-conductive states coexist at a given potential drop on the basis of the distribution of local electric fields.

In the non-conductive state, electric fields of most of ionized sites are weak (around zero) and those of neutral sites are strong, more than twice as strong as the external fields. Since, in our simulation, ionized sites are rejuvenated with a probability which depends on the strength of the electric field, ionized sites cannot be rejuvenated and they are neutralized. Therefore, the equilibrium of the non-conductive state is produced by the balance between creation and extinction of ionized sites without rejuvenation.

In the conductive state, rejuvenation of ionized sites occurs because the local electric field of each site is comparable with the external electric field. Thus ionized sites sustain the state by the rejuvenation which depends on the local electric field. Therefore, the equilibrium in the conductive state is produced by the balance between ionization of neutral sites and recombination of ionized sites which can be rejuvenated.

To see the effect of rejuvenation, we investigate the voltage dependence of the discharge when there is no rejuvenation ($a = b = 0$). Figure 9 shows the V dependence of the fraction of the ionized cells and the current flowing from the electrode. The fraction of ionized sites and the current do not show discontinuous changes when the applied voltage is increased.

A percolated cluster appears when the applied potential difference is increased. Since an ionized state is only neutralized by relaxation even if the local electric field is strong, the percolated cluster cannot be sustained and it remains for periods determined by the relaxation time. Thus, there is only the equilibrium caused by the balance between creation and extinction of ionized sites without sustaining ionized states. This indicates that the maintaining ionized sites caused by rejuvenation induces the discontinuous

transition of the discharge. Therefore rejuvenation of aged-ionized states plays an essential role for the discontinuous transition.

We note that the rejuvenation of ionized state in our simulation is indirectly caused by the local current because the local voltage drop is determined by the product of the local current and the local resistivity.

In conclusion, the nonlinear resistor network with three states shows a discontinuous transition when the applied potential difference is increased. The transition is similar to a first-order phase transition because non-conductive and conductive states can coexist at an applied potential drop. The discontinuous transition of the discharge is induced by rejuvenation of ionized states.

6. Theoretical Analysis of the Discontinuous Transition

6.1 Rate equation

We represent the reaction processes studied in Sects. 3, 4, and 5 by rate equations:

$$\frac{dN_{\rm F}}{dt} = \sum^{\rm N} F_i[f] - \sum^{\rm F} D_j[1-a] + \sum^{\rm A} B_k[b], \tag{9}$$

$$\frac{dN_{\rm A}}{dt} = \sum^{\rm F} D_j[1-a] - \sum^{\rm A}(B_k[b] + G_k[(1-b)g]), \tag{10}$$

$$\frac{dN_{\rm N}}{dt} = -\sum^{\rm N} F_i[f] + \sum^{\rm A} G_k[(1-b)g], \tag{11}$$

where $N_{\rm F}$, $N_{\rm A}$, and $N_{\rm N}$ denote the numbers of F, A, and N sites, F_i, D_j, B_k, and G_k denote the transition rates for N $\to$ F, F $\to$ A, A $\to$ F, and A $\to$ N, respectively, and $[\cdot]$ denotes that the transition rates are functions of parameters shown in Fig. 1(b). Because of the properties of F- and A-sites, the time evolution of the number of ionized sites can be written as follows:

$$\frac{dN_{\rm I}}{dt} = \sum^{\rm N} F_i[f] - \sum^{\rm A} G_k[(1-b)g], \tag{12}$$

where $N_{\rm I} = N_{\rm F} + N_{\rm A}$ is the total number of ionized sites. We analyze this equation on the basis of a mean field approach.

We rewrite Eq. (12) by averaging the transition rates:

$$\frac{1}{N_{\rm site}}\frac{dN_{\rm I}}{dt} = \frac{N_{\rm N}}{N_{\rm site}}\frac{1}{N_{\rm N}}\sum^{\rm F} F_i[f] - \frac{N_{\rm A}}{N_{\rm site}}\frac{1}{N_{\rm A}}\sum^{\rm A} G_k[(1-b)g], \tag{13}$$

where we divided both sides of the equation by the total number of sites, $N_{\rm site} = N_{\rm F} + N_{\rm A} + N_{\rm N}$. We also rewrite this equation as follows:

$$\frac{dp}{dt} = (1-p)\langle F_i\rangle_{\rm N} - p_{\rm A}\langle G_k\rangle_{\rm A}, \tag{14}$$

where $p = N_{\rm I}/N_{\rm site}$ is the fraction of ionized sites, and $p_{\rm A} = N_{\rm A}/N_{\rm site}$ is the fraction of aged ionized sites. We can obtain equilibrium states by the fixed point analysis ($dp/dt = 0$).

6.2 Mean field analysis

Since an A-site is a site which is not rejuvenated and not neutralized, we assume the fraction of aged-ionized sites and the averaged transition rates as follows:

$$\langle F_i\rangle_{\rm N} = we^{-E_0/\langle E_i\rangle_{\rm N}}, \tag{15}$$

$$\langle G_k\rangle_{\rm A} = 1/\tau, \tag{16}$$

$$p_{\rm A} = p(1 - e^{-E_0/\langle E_i\rangle_{\rm A}}), \tag{17}$$

where w is ionization rate of the medium and τ is the relaxation time. Thus, the equation to obtain the fixed point is given by

$$p = (1-p)\tau^* \frac{e^{-E_0/\langle E_i\rangle_{\rm N}}}{1 - e^{-E_0/\langle E_i\rangle_{\rm A}}}, \tag{18}$$

where $\tau^* \equiv \tau w$ is the scaled relaxation time.

We estimate the averaged electric field of resistor network in two-dimensional square lattice on the basis of a mean field approach.

When each site is equivalent after averaging, the perpendicular electric field, where the direction is perpendicular to the direction from one electrode to the other, is zero:

$$\langle E^x_{i,j}\rangle_c = 0, \tag{19}$$

and the parallel electric field is

$$\langle E^y_{i,j}\rangle_c = \left\langle \frac{i_{i,j-1}R_{i,j-1} + i_{i,j}R_{i,j}}{2\ell}\right\rangle = \frac{i_y}{\ell}\langle R_y\rangle, \tag{20}$$

where i_y is the uniform current flowing a resistor and R_y are a resistivity parallel to the direction from one electrode to the other. In an $N \times N$ resistor network, whole current is distributed into N channels. Therefore, the relation between the uniform current and whole current, $I(p, V)$, is given by

$$i_y = \frac{I(p,V)}{N}. \tag{21}$$

Thus, we express the averaged electric field using the current and averaged resistivity:

$$\langle E_{i,j}\rangle_c = \frac{I(p,V)}{N\ell}\langle R_y\rangle. \tag{22}$$

The strength of averaged electric field is required to coincide with that of the external field at $p = 0$ and 1.

We assume the current and averaged resistor as follows:

$$I(p,V) = \frac{N}{N+1}\frac{V}{r_0}\left(1 + \left(\frac{1}{\epsilon} - 1\right)p^\lambda\right), \tag{23}$$

$$\langle R_y(p)\rangle = r_0\left[\epsilon + (1-\epsilon)\frac{A(\zeta,\eta)}{e^{\eta(p-\zeta)}+1} + B(\zeta,\eta)\right], \tag{24}$$

where λ, ζ, and η are parameters, and r_0 is the resistivity of a resistor of non-conductive state. The current is determined so that it monotonically increases when p is increased and the derivative is zero at $p = 0$. For $\eta = \infty$, the resistivity behaves as a step function whose value is r_0 when $p < \zeta$ and ϵr_0 when $p > \zeta$. $A(\zeta,\eta)$ and $B(\zeta,\eta)$ are normalization constants of averaged resistivity so that $\langle R_y(p=0)\rangle = r_0$ and $\langle R_y(p=1)\rangle = \epsilon r_0$ ($\epsilon = 10^{-6}$ in the simulation):

$$A(\zeta,\eta) = \frac{(1+e^{-\eta\zeta})(e^{\eta(1-\zeta)}+1)}{e^{\eta(1-\zeta)} - e^{-\eta\zeta}}, \tag{25}$$

$$B(\zeta,\eta) = -\frac{1+e^{-\eta\zeta}}{e^{\eta(1-\zeta)} - e^{-\eta\zeta}}. \tag{26}$$

We determine the parameters so as to represent the effect of local structure of ionized region. Figure 10 shows the current, the averaged resistivity, and the averaged electric

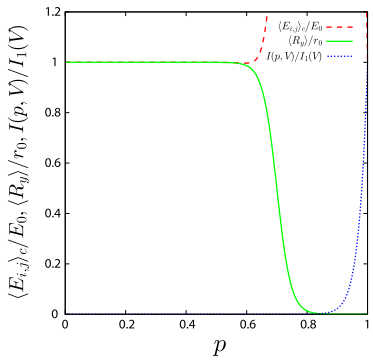

Fig. 10. (Color online) The averaged electric field, resistivity, and conductivity as a function of the fraction of ionized sites when $\lambda = 36$, $\zeta = 0.7$, and $\eta = 43$; red dashed line: the averaged electric field, green solid line: the resistivity, and blue dotted line: the current.

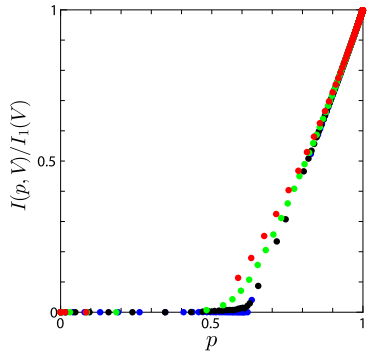

Fig. 11. (Color online) The conductivity of the resistor network as a function of the fraction of ionized sites for various relaxation times; The lowest series of dots (blue): $\tau/t_0 = 0.5$, the second lowest series of dots (black): $\tau/t_0 = 1.0$, the second series from the top (green): $\tau/t_0 = 3.0$, and the top series of dots (red): $\tau/t_0 = 10.0$. The data for $\tau/t_0 = 0.5$ and 1.0 are almost identical.

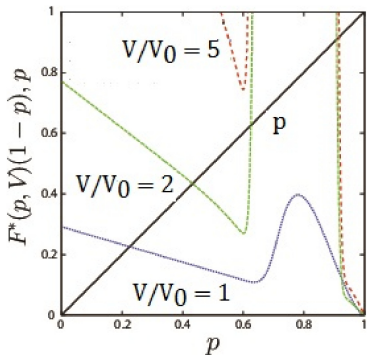

Fig. 12. (Color online) $F^*(p,V)(1-p)$ and p against the fraction of ionized sites at various voltage differences for $\tau^* = 0.5$; blue: $V/V_0 = 1.0$, green: $V/V_0 = 2.0$, red: $V/V_0 = 5.0$. The fractions of ionized sites at which a dashed line intersects with the solid line are fixed points at the applied potential difference.

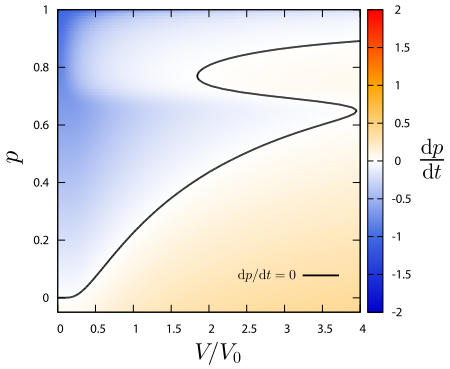

Fig. 13. (Color online) The voltage dependence of dp/dt for a given fraction of ionized sites for $\tau^* = 0.5$, where $\lambda = 36$ for Eq. (23), and $\zeta = 0.7$ and $\eta = 43$ for Eq. (24). The black solid curve represents $dp/dt = 0$, and $dp/dt > 0$ (< 0) on the right (left) hand side of the solid curve.

field as a function of the fraction of ionized sites where parameters are set to $\lambda = 36$, $\zeta = 0.7$, and $\eta = 43$. The conductivity obtained from Eq. (23) is smaller than that obtained from the simulation as shown in Fig. 11 in the range from $p = 0.5$ to 1.0. This effect is caused by the local structure of ionized region because most of the current flows through the percolated ionized region and therefore the current flowing neutral region, which affects the creation of ionized region, becomes smaller than the apparent current. Since there is virtually no rejuvenation of ionized sites before percolated clusters of ionized regions appear, we can assume that the averaged resistivity begins to decrease at the fraction of ionized sites where percolated clusters appear.

To obtain the fixed point of Eq. (14), we plot the left-hand and right-hand sides of Eq. (18) for $\tau^* = 0.5$ at various voltage differences as shown in Fig. 12, where $F^*(p,V)$ denotes the following function:

$$F^*(p,V) = \tau^* \frac{e^{-E_0/\langle E_i\rangle}}{(1 - e^{-E_0/\langle E_i\rangle})}. \tag{27}$$

The fraction of ionized sites at an intersection is a fixed point. There is a one fixed point when the external field is weak. There appear two fixed points as the external field exceeds a critical value. The number of fixed points becomes one again when the external filed is increased further. The voltage dependence of the fraction of ionized sites in the equilibrium state depends on the shape of $F^*(p,V)$ and the averaged electric field determines the equilibrium curve.

Figure 13 shows dp/dt [Eq. (14)] as a contour plot on the p–V plane for a given fraction of ionized sites and the applied voltage. The solid curve in Fig. 13 represents (V,p) at which $dp/dt = 0$. Therefore, the solid curve indicates the voltage dependence of the equilibrium state.

The equilibrium curve roughly reproduces the voltage dependence of the fraction of ionized sites obtained from the simulation in Sect. 3 for each relaxation time as shown in Figs. 13 and 14. Thus, it is important for understanding the discontinuous transition to take account of the local structure of ionized sites as discussed in Sect. 5.

In conclusion, we presented a mean field analysis of the discontinuous transition of the discharge. By incorporating the effect of the local structure of ionized region in the current, we obtained the equilibrium curve which reproduces the simulation results for different relaxation times.

7. Conclusion

In this paper, we presented a theoretical analysis of the discontinuous transition of the discharge in the nonlinear resistor network with consideration of rejuvenation of ionized states. The transition from non-conductive to conductive

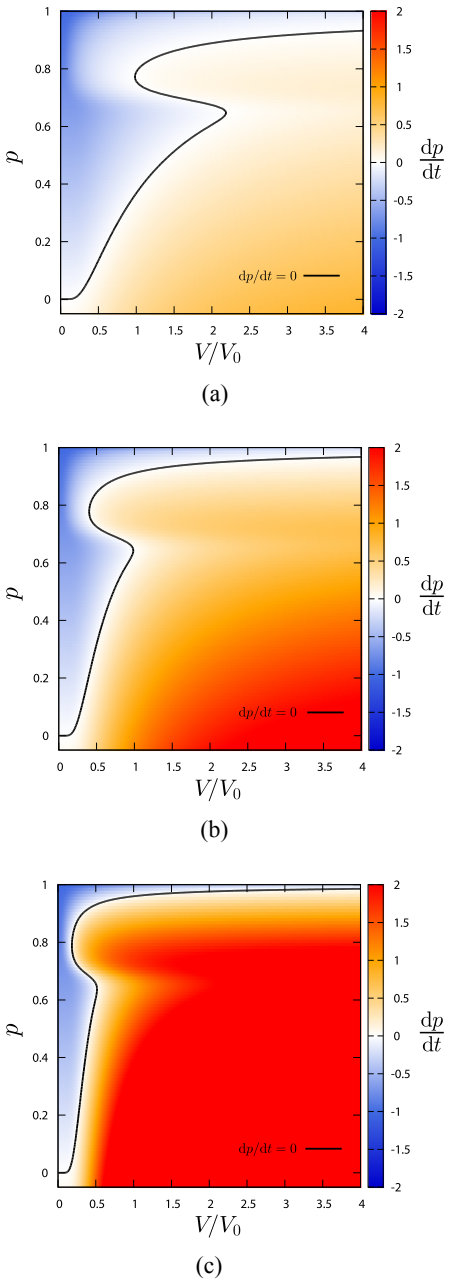

Fig. 14. (Color online) The voltage dependence of dp/dt for the given fraction of ionized sites for $\tau^* = 1.0$ (a), 3.0 (b), and 10.0 (c), where $\lambda = 36$ for Eq. (23), and $\zeta = 0.7$ and $\eta = 43$ for Eq. (24). The black solid curve represents $dp/dt = 0$, and $dp/dt > 0$ (< 0) on the right (left) hand side of the solid curve.

states when the applied potential difference is increased is similar to a first-order phase transition. The distribution of local electric fields fluctuates between non-conductive and conductive states. The variation of the distribution of local electric fields induces the change in the mechanism of equilibrating the states.

We also analyzed the discontinuous transition on the basis of a mean field approach. In the discontinuous transition, the physical quantities vary discontinuously when the voltage difference is increased. We noticed that the effect of local structure of ionized region is important for the transition. For more detailed analysist, it is necessary to take account of the cluster structure in averaging the local electric fields.

The model studied here is a coarse-grained model with the length scale ℓ and the results do not depend on the scale. Therefore, we expect that the discontinuous transition will be observed in any discharge phenomena including the lightning and the spark-plug.

The present results indicate that the discharge can be treated as transition phenomena in non-equilibrium system. The modeling and analyses can be applied not only to the discharge but also to other nonlinear phenomena by configuring the coarse-grained model and the interactions.

Acknowledgment We would like to thank Dr. A. Sasaki of JAEA for stimulating us to this research on discharge and for valuable comments throughout this research. We are also indebted to Drs. E. Takahashi and S. Katoh of AIST for valuable discussions and encouragement.

*t.odagaki@kb4.so-net.ne.jp

1) B. J. Munroe, A. M. Cook, M. A. Shapiro, R. J. Temkin, V. A. Dolgashev, L. L. Laurent, J. R. Lewandowski, A. D. Yeremian, S. G. Tantawi, and R. A. Marsh, Phys. Rev. ST Accel. Beams **16**, 012005 (2013).
2) S. Meijer, P. H. F. Morshuis, and J. J. Smit, Proc. 2004 IEEE Annual Report Conference on Electrical Insulation and Dielectric Phenomena, 2004.
3) M. Miki, T. Shindo, and Y. Aihara, J. Phys. D **29**, 1984 (1996).
4) Y. Shimada and S. Uchida, J. Plasma Fusion Res. **81** [Suppl.], 181 (2005).
5) H. Takayasu, Phys. Rev. Lett. **54**, 1099 (1985).
6) L. Niemeyer, L. Pietronero, and H. J. Wiesmann, Phys. Rev. Lett. **52**, 1033 (1984).
7) Y. Kishimoto and T. Masaki, J. Plasma Phys. **72**, 971 (2006).
8) A. Sasaki, Y. Kishimoto, E. Takahashi, S. Kato, T. Fujii, and S. Kanazawa, Phys. Rev. Lett. **105**, 075004 (2010).
9) S. Kato, E. Takahashi, A. Sasaki, and Y. Kishimoto, J. Plasma Fusion Res. **84**, 477 (2008).
10) S. Matsumoto and T. Odagaki, J. Phys. Soc. Jpn. **83**, 034006 (2014).
11) Y. P. Raizer, *Gas Discharge Physics* (Springer, Berlin/Heidelberg, 1991) Chap. 4, p. 56.